Ultrafast Processes for Bulk Modification of Transparent Materials

Kazuyoshi Itoh, Wataru Watanabe, Stefan Nolte, and Chris B. Schaffer

Abstract

When a femtosecond laser pulse is focused inside a transparent material, the optical intensity in the focal volume can become high enough to induce permanent structural modifications such as a refractive index change or the formation of a small vacancy. Thus, one can micromachine structures inside the bulk of a transparent material in three dimensions. We review the mechanisms of and techniques for bulk modification of transparent materials using femtosecond laser pulses and discuss the fabrication of photonic and other structures in transparent materials, including waveguides, couplers, gratings, diffractive lenses, optical data storage, and microfluidic channels.

Keywords: *fluidics, laser, machining, optical.*

Introduction

Ultrafast lasers have extremely short pulse durations or, equivalently, extremely wide signal bandwidth. While the latter feature enables ultrafast photonic communications channels, the former promises the fabrication of integrated photonic communications and signal processing systems inside transparent materials. The extraordinarily high peak power of short-duration optical pulses provides a new approach for local modification of transparent materials through nonlinear optical processes.

Recent demonstrations of three-dimensional (3D) micromachining of glass using ultrafast laser pulses include the fabrication of waveguides, couplers, gratings, binary data storage devices, lenses, and channels. Thus, direct-writing of optical devices using ultrafast laser pulses has potential applications in the telecommunications and optical signal processing industries. The most important feature of this microfabrication technique is its ability to integrate 3D optical or photonic devices inside transparent materials by sequential direct-writing of individual devices. Although such a sequential approach is slow in comparison with conventional lithography, the new capability for 3D integration is priceless, in that it is quite difficult to achieve by other methods.

Although mechanisms for ultrafast-laser-induced structural changes are not yet well understood, the current understanding will be reviewed here, followed by demonstrations of the fabrication of photonic devices and microfluidic channels. Recent advances, especially in writing waveguides using megahertz oscillators without the use of regenerative amplifiers, are discussed at the end of this article.

Mechanisms for Femtosecond-Laser-Induced Structural Change

When an intense femtosecond laser pulse is tightly focused inside the bulk of a transparent material (Figure 1a), the intensity in the focal volume can become high enough to initiate absorption through nonlinear field ionization (multiphoton absorption and tunneling ionization) and avalanche ionization, in which one electron gains energy from the laser field and impact-ionizes an additional electron (Figure 1b).[1–5] This nonlinear absorption results in the creation of an electron-ion plasma that is localized to the focal volume (Figure 1c). As the plasma recombines and its energy is dissipated, permanent structural changes can be induced in the material (Figure 1d). Because the nonlinear absorption allows energy to be deposited into the bulk of a transparent material, these structural changes can be produced inside the sample without affecting the surface, allowing 3D structures to be fabricated by translating the laser focus through the sample.

To date, three qualitatively different kinds of structural changes have been induced in the bulk of transparent materials with femtosecond laser pulses: an isotropic refractive index change;[6,7] a birefringent refractive index change;[8,9] and a void[10–12] (Figure 1d). The structure produced depends on laser parameters (pulse duration, wavelength, energy, repetition rate), material parameters (bandgap, thermal expansion coefficient, etc.), and the numerical aperture (NA) of the focusing. In the case of tightly focused (NA ~ 0.65), 100-fs, 800-nm pulses in fused silica, each of the three morphologies can be produced by just varying the incident laser energy.

The isotropic refractive index changes observed at near-threshold energy have been attributed to localized melting and rapid resolidification of the glass.[13–15] In fused silica, the density and refractive index of the material is higher if the glass is quenched from a higher temperature.[16,17] Thus, if the material in the focal volume melts, then quenches, we expect a higher refractive index and higher density in the irradiated region for fused silica than in a non-irradiated region. Indeed, Raman microspectroscopy measurements indicate an increase in the number of 3- and 4-member ring structures in the silica network following femtosecond laser irradiation, while 5- and 6-member rings predominate in untreated glass. This increase in the number of smaller rings is consistent with densification.[13,15] Additionally, infrared spectroscopy indicates a change in the Si–O–Si bond angle, indicative of densification.[18] Finally, many groups have observed that lines written in fused silica by translating the laser focus through the glass form single-mode optical waveguides, implying a higher refractive index in the irradiated area.[19–21] Glasses that display more typical thermal behaviors (meaning the density and refractive index decrease as the glass is quenched from higher temperatures) such as the phosphate glass IOG-1 (Schott Inc.) show a lower refractive index and lower density

https://doi.org/10.1557/mrs2006.159

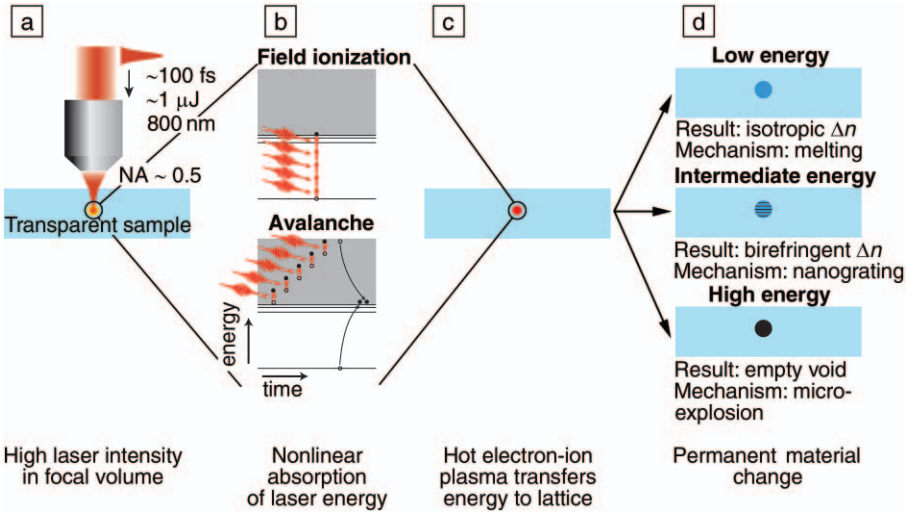

Figure 1. Schematic illustration of key steps in femtosecond-laser-induced structural change in bulk transparent materials. (a)–(c) A hot electron-ion plasma is formed in the focal volume through nonlinear absorption of intense femtosecond laser pulses. (d) Depending on the amount of energy contained in the plasma, three different types of structural change can occur: isotropic refractive index change at low energy, birefringent refractive index change at intermediate energy, or void formation at high energy.

in the femtosecond-laser-irradiated region.[14] From this evidence, it seems likely that near-threshold femtosecond laser irradiation leads to heating and melting of the glass in the focal volume; this glass subsequently rapidly cools and freezes-in the properties of the higher-temperature state. In fused silica, 100-fs, 800-nm pulses focused at a 0.65 NA produce an isotropic refractive index change for laser energies of 40–150 nJ.

Only recently have clues to the birefringent refractive index changes observed at intermediate energy[8,9] been uncovered. Shimotsuma et al. found that periodic, nanometer-scale stripes with varying material composition are formed in the irradiated volume, with the stripes oriented perpendicular to the polarization of the femtosecond laser beam.[22] Backscattered-electron scanning electron microscopy images reveal that in fused silica the stripes consist of alternating layers of material, approximately 20 nm in width, with layers of slightly higher than normal density alternating with layers of much lower than normal density.[22] Auger spectra maps reveal that the low-density regions are depleted in oxygen, while the silicon concentration seems unaffected throughout the structure.[22] In TeO_2, the stripes consist of alternating layers of nanometer-scale voids and relatively undamaged material.[23] These nanometer-scale variations in material density and composition, termed a "nanograting," give rise to birefringence in the structures.[24] It has also been found that in fused silica the lower-density stripes of the nanograting can be etched by hydrofluoric acid (HF) almost 300 times faster than unmodified material, again indicating large differences in the material properties in alternate stripes of the nanograting.[25,26]

The mechanism proposed to explain the formation of the nanogratings involves interference between the femtosecond laser field and the electric field of bulk electron plasma waves in the laser-produced plasma. This interference leads to periodic modulations in the electron plasma density, which in turn lead to periodic modulations in the degree of structural change produced.[22] For example, interstitial oxygen atoms produced in greater number in the high-electron-density regions could diffuse away, leaving the observed oxygen-deficient zones.[23] In fused silica, 100-fs, 800-nm pulses focused at 0.65 NA produce birefringent refractive index changes for laser energies of 150–500 nJ.

Voids produced at high energy are attributed to an explosive expansion of highly excited, vaporized material out of the focal volume and into the surrounding material, a process termed a microexplosion.[10,11,27] Because this expansion occurs within the bulk of the material, the microexplosion leaves a less dense or hollow core (void) surrounded by a densified shell of material.[12,28] For 100-fs, 800-nm pulses focused at a 0.65 NA, voids are observed for energies of >500 nJ in fused silica.

Other processes are also known to occur during structural changes in the bulk of a transparent material by femtosecond laser irradiation. For example, E′ color centers (positively charged oxygen vacancies) and nonbridging oxygen hole centers are formed in fused silica.[15,19] These defects, however, are known not to make a major contribution to the refractive index change in the structure because samples that have been thermally annealed to eliminate these defects do not revert to the original refractive index.[21,29] In multicomponent glasses, migration of components may also play a role in producing a refractive index change, even in the low-energy regime where smooth refractive index profiles are produced.[30]

Our discussion of the structural changes induced by femtosecond pulses strictly applies only to structural changes induced by single laser pulses, but likely describes the changes induced by multiple laser pulses arriving at the same spot, provided that the repetition rate is low enough that all thermal and mechanical relaxation processes are completed between laser pulses. In this case, subsequent pulses may add to the structural change that is produced, but each pulse acts more or less independently to alter the material.

For high repetition rates, where the material does not fully relax between pulses, pulse-to-pulse cumulative effects can play a role. For example, when the repetition rate becomes higher than the inverse of the characteristic time for energy to thermally diffuse out of the focal region, heat will accumulate in the focal volume as energy from more and more pulses is absorbed;[31–33] the laser serves as a localized source of heat within the material.[34] In this case, the morphology of the structural change will be dominated by the heating, melting, and cooling dynamics of the material in and around the focal volume. A volume of material much greater than the focal volume can be structurally altered, because if enough energy is absorbed, a volume of material larger than the focal volume can be heated above the melting temperature. After the laser pulse train is turned off, the heated material rapidly cools, freezing-in the density and other structural properties of the high-temperature state. In fused silica, this leads to a large increase in refractive index of up to 1%.[35,36]

The dynamics of the cooling may also help determine the profile of the refractive index change. For example, a borosilicate glass will freeze in a lower-density state when quenched from high temperature. A high-repetition-rate femtosecond laser

https://doi.org/10.1557/mrs2006.159

train will melt a roughly spherical volume inside the bulk of such a glass. When this volume cools, the outer regions will freeze in the lower-density state, but because this occurs in the bulk where no free surface can expand, the central part of the melted volume will cool under pressure, in some cases leading to an increase in the density and refractive index.[34]

We have provided a guide to current thinking about the dominant mechanisms for producing structural changes in transparent materials with femtosecond optical pulses. There are other possibilities, however. While the thermal mechanism seems likely, the isotropic refractive index change observed at low laser energy could be caused by direct photostructural transitions. For example, ultraviolet laser pulses are known to induce densification in fused silica through ionization of the glass,[37] and femtosecond laser irradiation may ionize the same bonds through nonlinear absorption and induce densification. The role of induced stress has also not been fully explored.[20,29] Although much progress has been made in identifying the mechanisms for producing the structures used for waveguide writing and other micromachining applications, more research is necessary before our understanding can be considered adequate.

Fabrication of Photonic Devices

Optical Memory

As an application of void formation in transparent materials, 3D optical data storage has been reported, with the occurrence of a void representing a binary value of 1, and the absence of a void a binary 0.[10,27] The position of the void can be changed by the same femtosecond laser pulses.[38,39] After the formation of a void, a microexplosion likely occurs near the front interface of the void by shifting the focal region. Defects and easily ionized surface states near the interface may enhance the breakdown process. When a microexplosion occurs at this front interface, the debris from the new void fills in the old void, and the void moves in an upstream direction. Lateral movement of the void along the axis perpendicular to the beam propagation axis was achieved by shifting the focus of the laser pulses.[39]

Waveguides and Couplers

For the fabrication of waveguides, a localized, single-point modification, typically in the regime where isotropic refractive index changes are produced, must be extended to a line. This is commonly accomplished by moving the focus through the sample, either parallel to or transverse to the axis of the laser beam. The former technique offers the advantage that the waveguides will be circular in shape;[6] however, the working distance of the objective lens limits the writing length of the waveguide. Thus, low-NA objectives with a long working distance (the distance between the front lens of the objective and the point of focus) are needed to produce waveguides with a length of a few centimeters. Such focusing conditions also offer the potential for the generation of beam filamentation and the production of waveguides without moving the focus.[40]

The transverse writing geometry is more flexible. Structures can be fabricated within the bulk material, limited in size only by the positioning system, while the maximum structure depth is determined by the working distance of the focusing objective. The main disadvantage, however, is the asymmetry of the produced structure. Except for very high-NA objectives, the focal radius will always be much smaller than the confocal parameter, resulting in a waveguide with an elliptical cross section.[21] To obtain waveguides with a circular cross section, Osellame et al.[41] have suggested using an elliptical writing beam. In combination with movement of the focus, circular waveguides can be obtained. This has been demonstrated by beam shaping,[42] and in a simpler setup (however, at the expense of energy loss) by using a slit in front of the focusing objective.[43]

Using these approaches, waveguides have been written in various glasses,[6,19] actively doped glasses,[44–47] crystals,[28,48–50] and polymers.[51,52] The change in refractive index obtained depends on the pulse energy[53] and the number of pulses applied (i.e., the writing speed).[21] Thus, single- or multimode waveguides can be produced by changing the writing parameters. Transmission losses of < 0.4 dB/cm have been reported,[54,55] suitable for most integrated optics applications.

Femtosecond direct-writing allows true 3D structuring. Consequently, couplers and splitters have been reported not only in 2D[53,56] but also in 3D.[57–59] They can be fabricated by simply moving the focus along the desired paths. The 3D capabilities offer the potential for higher packing density and the realization of more complex functions; for example, crossings can easily be avoided in a 3D architecture. One example for a higher density of optical functions is to stack waveguides into an array,[32] where the third dimension is used to increase the packaging density. However, if the waveguides are stacked closer together, the evanescent field will be able to couple to adjacent waveguides. Thus, the structure can no longer be described as a collection of single waveguides but must be treated as a whole. As a consequence, the glass substrate will no longer show standard diffraction behavior when exposed to light but will show the peculiar features of discrete diffraction.[60,61] Note that the realization of such an array of coupled waveguides requires a high homogeneity of the refractive index changes induced in each waveguide, since even small deviations in phase between the waveguides will result in a significantly altered intensity distribution at the exit of the device.

Gratings

Gratings are fabricated in glass by direct-writing.[7,8] Sudrie et al. fabricated birefringent gratings in bulk silica using birefringent refractive index changes.[7] The grating was written by 2D displacement of a silica glass sample perpendicular to the beam propagation axis. A grating with a period of 6 μm and a thickness of 20 μm had a diffraction efficiency of 20%. A volume grating with a thickness of 300 μm and a period of 3 μm was fabricated in silica glass using isotropic refractive index changes, and a diffraction efficiency of 74.8% (compared with the theoretical optimum value of 100%) was achieved.[62]

The other method of fabricating gratings with femtosecond laser pulses is the two-beam interference method. In conventional holography, an optical interference pattern of two coherent laser beams is stored on or within a photosensitive optical medium such as photorefractive crystals or photopolymers. A surface-relief grating with a period of < 1 μm can be encoded on the surface of nonphotosensitive glasses by two-beam interference of a single near-infrared femtosecond laser pulse.[63] Using this technique, holographic gratings can also be fabricated inside glass.[64,65] Holographic data storage was demonstrated on the surface of fused silica, soda-lime glass, lead glass, and polymers by two-beam interference of a single femtosecond laser pulse.[66,67]

Lenses

Techniques for fabricating diffractive lenses can be divided into two categories: amplitude-type and phase-type. The amplitude-type diffractive lens, also called a Fresnel zone plate, can be fabricated by embedding voids in silica glass. When either all the even or all the odd zones are blocked, the zone plate has a focusing property. Such an amplitude-type diffractive lens, with an efficiency of ~2% at a wavelength of 632.8 nm, was realized by embedding voids in silica glass; the

https://doi.org/10.1557/mrs2006.159

maximum theoretical diffraction efficiency is $1/\pi^2 = 10.1\%$.[68]

On the other hand, the phase-type diffractive lens, also called a kinoform, utilizes all the incident light and therefore achieves a higher diffraction efficiency. The lens consists of a series of disks centered at one point, forming alternating annular zones with different refractive indexes. The fabrication of two-level phase-type diffractive lenses was demonstrated by inducing a birefringent refractive index change in silica glass.[24] The efficiency of this lens reached ~40% at a wavelength of 404 nm and is dependent on the polarization of an incident beam. Birefringence-free diffractive lenses were demonstrated in silica glass by inducing isotropic refractive index changes.[69] The design of a four-level lens is shown in Figure 2a. Side and top views of the fabricated lens are shown in Figures 2b and 2c, respectively. The resolution of this lens was 9.9 μm, and an efficiency of 56.9% was achieved.

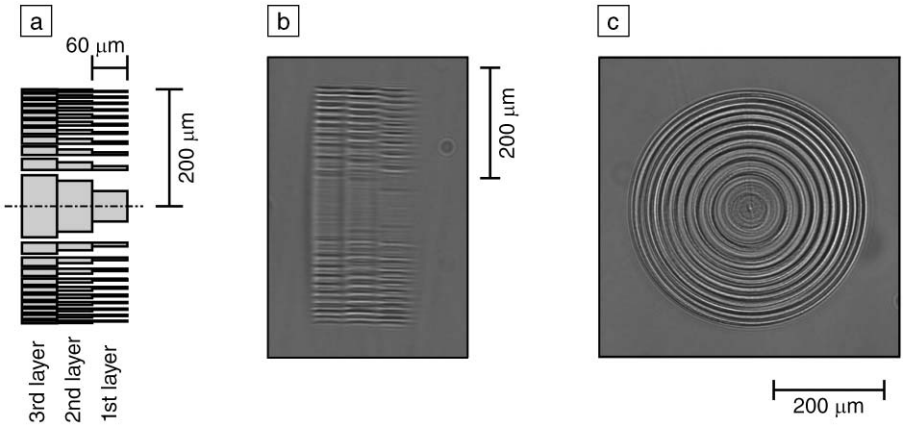

Figure 2. (a) Design of a four-level phase-type diffractive lens (fourth layer is not visible here). (b) Side view of fabricated lens. (c) Top view of lens.

Fabrication of Microfluidic Channels

It is possible to fabricate hollow, micrometer-diameter channels that have a 3D arrangement in the bulk of a transparent material with femtosecond laser pulses, opening the door to direct-writing of microfluidic devices. Two approaches for manufacturing microfluidic channels with a 3D architecture have been demonstrated to date.

The first method takes advantage of the increase in HF etch rate for glass, where femtosecond laser irradiation has led to the production of nanogratings.[25,26] A pattern of damage lines is written into the sample using laser energies in the intermediate regime, where nanogratings are formed. The sample is then immersed in a dilute solution of HF. The laser-modified tracks etch much faster than the unmodified glass, leading to the formation of hollow channels that lie along the laser-produced damage lines.[70–73] This technique has been used to fabricate active microfluidic devices.[74]

The second method relies on the void formation mechanism that dominates at high energy, with many voids linked together to form a hollow channel. When machining high-aspect-ratio channels with this method, debris removal becomes a problem—channel openings are clogged by debris produced while drilling deeper. To alleviate the debris removal problem, a wetting fluid is introduced that wicks into the laser-drilled channels during their formation and carries away the debris.[75] This technique has been demonstrated in glass[75–77] and polymer materials[78] (Figure 3); channel diameters as small as 0.5 μm have been demonstrated.[77,78]

In both techniques, the fabrication speed is relatively slow, so it is advantageous to produce as much of the device as possible using standard soft lithography or molding and then go back and laser-machine channels that, because of their shape or location, cannot be fabricated using standard techniques[78] (Figure 3). The integration of microfluidic channels and optical waveguides into a single device may enable "lab-on-a-chip" applications with greater functionality.

Recent Advances

Despite the promising results and applications discussed here, a drawback of this technology is the limited processing speed. This drawback can be overcome by using a high-repetition-rate writing laser system, for example, a femtosecond oscillator with an elongated cavity that increases the pulse energy.[31] In combination with tight focusing objectives, these systems have sufficient pulse energy to create the required refractive index changes.[31–34,51] Femtosecond oscillators or simple amplifier systems producing >100 nJ pulse energy at megahertz

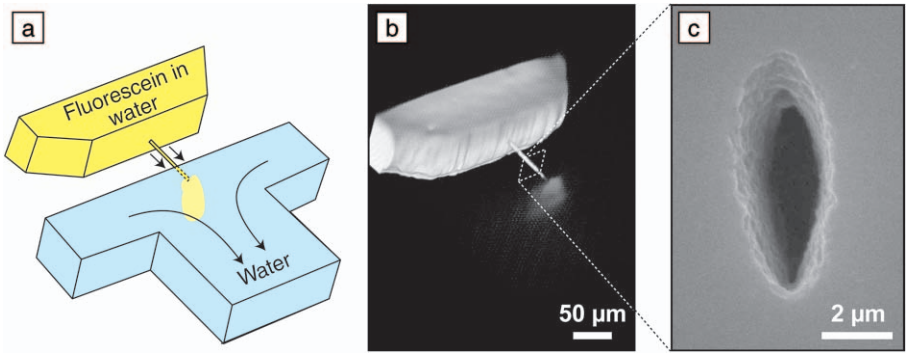

Figure 3. A femtosecond-laser-drilled microcapillary integrated into a molded microfluidic device made of poly(dimethylsiloxane) (PDMS). (a) Schematic illustration of a molded and drilled channel: A microcapillary is drilled between the molded channel at the top and the molded T-shaped channel below. To visualize flow through the microcapillary, the channel at the top is filled with a solution of fluorescein in water, while the T-shaped channel is filled with pure water. When the pressure in the top channel is higher than in the T-channel, the fluorescein solution flows through the microcapillary into the T-channel. The arrows show the direction of flow through the microcapillary and in the T-channel. (b) Rendered two-photon fluorescence microscopy image stack of the flow of a solution of fluorescein in water through a femtosecond-laser-drilled microcapillary. (c) Scanning electron microscopy image of the opening of the microcapillary, showing the small size and smooth walls of the channels. The channel was drilled in bulk PDMS with 27-nJ, 800-nm, 100-fs laser pulses focused at 1.0 NA. Data adapted from Reference 46.

https://doi.org/10.1557/mrs2006.159

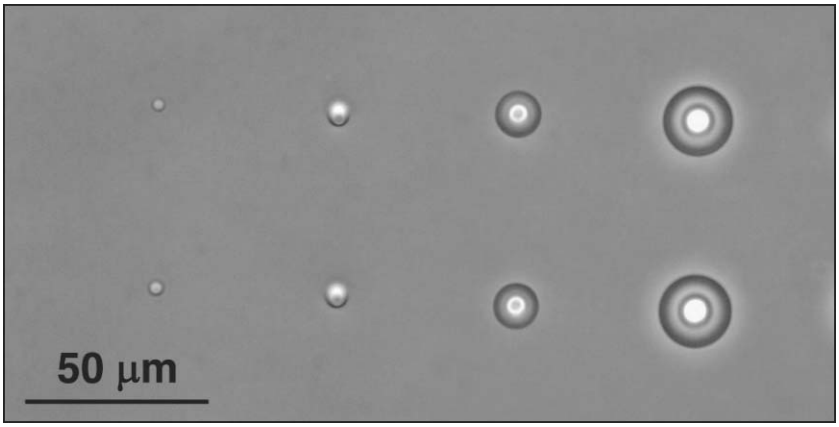

Figure 4. Optical microscope image of structures produced with multiple 5-nJ, 30-fs laser pulses from a 25-MHz oscillator focused by a 1.4 NA objective. The laser pulses are incident perpendicular to the plane of the image, and the number of pulses incident on the sample increases, by factors of 10, from 10^2 on the left to 10^5 on the right.

repetition rates are commercially available. This allows the production of waveguides with relaxed focusing conditions in a compact and reliable setup.[47,79] Writing speeds of up to 100 mm/s have been reported, limited only by the positioning system.[55] Such high processing speeds greatly mitigate any disadvantage of serial processing.

However, when machining at such high repetition rates, the mechanisms of modification change, as detailed earlier. As a consequence, the size of the induced modifications depends not only on the focusing conditions but also on the pulse energy and on the number of pulses applied (Figure 4).

Another interesting property of the modified structures is the nonlinear response. Until recently, only the linear response of femtosecond-written waveguiding structures has been investigated. However, Zoubir et al.[80] and Szameit et al.[81] noticed that the femtosecond laser pulses modified not only the linear index of refraction but also the nonlinearity. A reduction in the nonlinear refractive index n_2 of up to 70% was observed.[80,81] Thus, by careful control of the processing parameters, one can adapt the nonlinear refractive index to the experimental requirements as an additional degree of freedom.

In combination with an array of closely stacked waveguides, the nonlinear dynamics are of particular interest. Due to the nonlinear response of the medium, the coupling conditions will change for different input powers.[81] As a consequence, so-called discrete spatial solitons can be generated that do not undergo diffraction with propagation. This has been an intensely studied research topic using conventional integrated optics. With the new degrees of freedom enabled by 3D structuring using femtosecond-laser direct-writing, novel routing[82] and switching[83] concepts may become possible.

References

1. B.C. Stuart, M.D. Feit, S. Herman, A.M. Rubenchik, B.W. Shore, and M.D. Perry, *Phys. Rev. B* **53** (1996) p. 1749.
2. M. Lenzner, J. Krüger, S. Sartania, Z. Cheng, Ch. Spielmann, G. Mourou, W. Kautek, and F. Krausz, *Phys. Rev. Lett.* **80** (1998) p. 4076.
3. D. Du, X. Liu, G. Korn, J. Squier, and G. Mourou, *Appl. Phys. Lett.* **64** (1994) p. 3071.
4. C.B. Schaffer, A. Brodeur, and E. Mazur, *Meas. Sci. Technol.* **12** (2001) p. 1784.
5. A.P. Joglekar, H.-H. Liu, E. Meyhöfer, G. Mourou, and A.J. Hunt, *Proc. Natl. Acad. Sci. USA* **101** (2004) p. 5856.
6. K. Miura, J. Qiu, H. Inouye, T. Mitsuyu, and K. Hirao, *Appl. Phys. Lett.* **71** (1997) p. 3329.
7. C. Florea and K.A. Winick, *J. Lightwave Technol.* **21** (2003) p. 246.
8. L. Sudrie, M. Franco, B. Prade, and A. Mysyrowicz, *Opt. Commun.* **171** (1999) p. 279.
9. L. Sudrie, M. Franco, B. Prade, and A. Mysyrowicz, *Opt. Commun.* **191** (2001) p. 333.
10. E.N. Glezer, M. Milosavljevic, L. Huang, R.J. Finlay, T.-H. Her, J.P. Callan, and E. Mazur, *Opt. Lett.* **21** (1996) p. 2023.
11. E.N. Glezer and E. Mazur, *Appl. Phys. Lett.* **71** (1997) p. 882.
12. C.B. Schaffer, A.O. Jamison, and E. Mazur, *Appl. Phys. Lett.* **84** (2004) p. 1441.
13. J.W. Chan, T. Huser, S. Risbud, and D.M. Krol, *Opt. Lett.* **26** (2001) p. 1726.
14. J.W. Chan, T.R. Huser, S.H. Risbud, J.S. Hayden, and D.M. Krol, *Appl. Phys. Lett.* **82** (2003) p. 2371.
15. J.W. Chan, T.R. Huser, S.H. Risbud, and D.M. Krol, *Appl. Phys. A* **76** (2003) p. 367.
16. R. Bruckner, *J. Non-Cryst. Solids* **5** (1970) p. 123.
17. R. Bruckner, *J. Non-Cryst. Solids* **6** (1971) p. 177.
18. K. Kawamura, N. Sarukura, M. Hirano, and H. Hosono, *Appl. Phys. Lett.* **78** (2001) p. 1038.
19. K.M. Davis, K. Miura, N. Sugimoto, and K. Hirao, *Opt. Lett.* **21** (1996) p. 1829.
20. D. Homoelle, W. Wielandy, A.L. Gaeta, E.F. Borrelli, and C. Smith, *Opt. Lett.* **24** (1999) p. 1311.
21. M. Will, S. Nolte, B.N. Chichkov, and A. Tünnermann, *Appl. Opt.* **41** (2002) p. 4360.
22. Y. Shimotsuma, P.G. Kazansky, J. Qiu, and K. Hirao, *Phys. Rev. Lett.* **91** 247405 (2003).
23. Y. Shimotsuma, K. Hirao, J. Qiu, and P.G. Kazansky, *Mod. Phys. Lett. B* **19** (2005) p. 225.
24. E. Bricchi, B.G. Klappauf, and P.G. Kazansky, *Opt. Lett.* **29** (2004) p. 119.
25. C. Hnatovsky, R.S. Taylor, P.P. Rajeev, E. Simova, V.R. Bhardwaj, D.M. Rayner, and P.B. Corkum, *Appl. Phys. Lett.* **87** (2005) p. 14104.
26. C. Hnatovsky, R.S. Taylor, E. Simova, V.R. Bhardwaj, D.M. Rayner, and P.B. Corkum, *Opt. Lett.* **30** (2005) p. 1867.
27. J.R. Qiu, K. Miura, and K. Hirao, *Jpn. J. Appl. Phys. Part 1* **37** (1998) p. 2263.
28. T. Gorelik, M. Will, S. Nolte, A. Tünnermann, and U. Glatzel, *Appl. Phys. A* **76** (2003) p. 309.
29. A.M. Streltsov and N.F. Borrelli, *J. Opt. Soc. Am. B* **19** (2002) p. 2469.
30. V.R. Bhardwaj, E. Simova, P.B. Corkum, D.M. Rayner, C. Hnatovsky, R.S. Taylor, B. Schreder, M. Kluge, and J. Zimmer, *J. Appl. Phys.* **97** 083102 (2005).
31. C.B. Schaffer, A. Brodeur, J.F. Garcia, and E. Mazur, *Opt. Lett.* **26** (2001) p. 93.
32. K. Minoshima, A.M. Kowalevicz, I. Hartl, E.P. Ippen, and J.G. Fujimoto, *Opt. Lett.* **26** (2001) p. 1516.
33. K. Minoshima, A.M. Kowalevicz, E.P. Ippen, and J.G. Fujimoto, *Opt. Express* **10** (2002) p. 645.
34. C.B. Schaffer, J.F. Garcia, and E. Mazur, *Appl. Phys. A* **76** (2003) p. 351.
35. M. Will, J. Burghoff, J. Limpert, T. Schreiber, S. Nolte, and A. Tünermann, in *Conference on Lasers and Electro-Optics (CLEO)*, edited by A.A. Sawchuk (Optical Society of America, Baltimore, MD, 2003) paper No. CWI 6.
36. L. Shah, A.Y. Arai, S.M. Eaton, and P.R. Herman, *Opt. Express* **13** (2005) p. 1999.
37. N.F. Borrelli, C. Smith, D.C. Allan, and T.P. Seward, *J. Opt. Soc. Am. B* **14** (1997) p. 1606.
38. W. Watanabe, T. Toma, K. Yamada, J. Nishii, K. Hayashi, and K. Itoh, *Opt. Lett.* **25** (2000) p. 1669.
39. W. Watanabe and K. Itoh, *Opt. Express* **10** (2002) p. 603.
40. K. Yamada, W. Watanabe, T. Toma, K. Itoh, and J. Nishii, *Opt. Lett.* **26** (2001) p. 19.
41. R. Osellame, S. Taccheo, M. Marangoni, R. Ramponi, P. Laporta, D. Polli, S. De Silvestri, and G. Cerullo, *J. Opt. Soc. Am. B* **20** (2003) p. 1559.
42. G. Cerullo, R. Osellame, S. Taccheo, M. Marangoni, D. Polli, R. Ramponi, P. Laporta, and S. De Silvestri, *Opt. Lett.* **27** (2002) p. 1938.
43. M. Ams, D.J. Spence, G.D. Marshall, and M.J. Withford, *Opt. Express* **13** (2005) p. 5676.
44. Y. Sikorski, A.A. Said, P. Bado, R. Maynard, C. Florea, and K.A. Winick, *Electron. Lett.* **36** (2000) p. 226.
45. R. Osellame, S. Taccheo, G. Cerullo, M. Marangoni, D. Polli, R. Ramponi, P. Laporta, and S. De Silvestri, *Electron. Lett.* **38** (2002) p. 964.

https://doi.org/10.1557/mrs2006.159

46. S. Taccheo, G. Della Valle, R. Osellame, G. Cerullo, N. Chiodo, P. Laporta, O. Svelto, A. Killi, U. Morgner, M. Lederer, and D. Kopf, *Opt. Lett.* **29** (2004) p. 2626.
47. R. Osellame, N. Chiodo, G. Della Valle, S. Taccheo, R. Ramponi, G. Cerullo, A. Killi, U. Morgner, M. Lederer, and D. Kopf, *Opt. Lett.* **29** (2004) p. 1900.
48. L. Gui, B. Xu, and T.C. Chong, *IEEE Photon. Technol. Lett.* **16** (2004) p. 1337.
49. V. Apostolopoulos, L. Laversenne, T. Colomb, C. Depeursinge, R.P. Salathé, M. Pollnau, R. Osellame, G. Cerullo, and P. Laporta, *Appl. Phys. Lett.* **85** (2004) p. 1122.
50. A.H. Nejadmalayeri, P.R. Herman, J. Burghoff, M. Will, S. Nolte, and A. Tünnermann, *Opt. Lett.* **30** (2005) p. 964.
51. A. Zoubir, M. Richardson, C. Rivero, A. Schulte, C. Lopez, K. Richardson, N. Hô, and R. Valle, *Opt. Lett.* **29** (2004) p. 748.
52. S. Sowa, W. Watanabe, J. Nishii, and K. Itoh, *Opt. Express* **14** (2006) p. 291.
53. D. Homoelle, S. Wielandy, A.L. Gaeta, N.F. Borrelli, and C. Smith, *Opt. Lett.* **24** (1999) p. 1311.
54. S. Nolte, M. Will, J. Burghoff, and A. Tünnermann, *J. Mod. Opt.* **51** (2004) p. 2533.
55. Y. Nasu, M. Kohtoku, and Y. Hibino, *Opt. Lett.* **30** (2005) p. 723.
56. A.M. Streltsov and N.F. Borrelli, *Opt. Lett.* **26** (2001) p. 42.
57. W. Watanabe, T. Asano, K. Yamada, K. Itoh, and J. Nishii, *Opt. Lett.* **28** (2003) p. 2491.
58. S. Nolte, M. Will, J. Burghoff, and A. Tünnermann, *Appl. Phys. A* **77** (2003) p. 109.
59. A.M. Kowalevicz, V. Sharma, E.P. Ippen, J.G. Fujimoto, and K. Minoshima, *Opt. Lett.* **30** (2005) p. 1060.
60. T. Pertsch, U. Peschel, F. Lederer, J. Burghoff, M. Will, S. Nolte, and A. Tünnermann, *Opt. Lett.* **29** (2004) p. 468.
61. A. Szameit, D. Blömer, J. Burghoff, T. Pertsch, S. Nolte, and A. Tünnermann, *Appl. Phys. B* **82** (2006) p. 507.
62. K. Yamada, W. Watanabe, J. Nishii, and K. Itoh, *Jpn. J. Appl. Phys., Part 1* **42** (2003) p. 6916.
63. K. Kawamura, T. Ogawa, N. Sarukura, M. Hirano, and H. Hosono, *Appl. Phys. B* **71** (2000) p. 119.
64. Y. Li, W. Watanabe, K. Itoh, and X. Sun, *Appl. Phys. Lett.* **81** (2002) p. 1952.
65. K. Kawamura, T. Ogawa, N. Sarukura, M. Hirano, and H. Hosono, *Appl. Phys. B* **71** (2000) p. 119.
66. Y. Li, W. Watanabe, K. Yamada, T. Shinagawa, K. Itoh, J. Nishii, and Y. Jiang, *Appl. Phys. Lett.* **80** (2002) p. 1508.
67. Y. Li, K. Yamada, T. Ishizuka, W. Watanabe, K. Itoh, and Z. Zhou, *Opt. Express* **10** (2002) p. 1173.
68. W. Watanabe, D. Kuroda, K. Itoh, and J. Nishii, *Opt. Express* **10** (2002) p. 978.
69. K. Yamada, W. Watanabe, Y. Li, K. Itoh, and J. Nishii, *Opt. Lett.* **29** (2004) p. 1846.
70. A. Marcinkevièius, S. Juodkazis, M. Watanabe, M. Miwa, S. Matsuo, H. Misawa, and J. Nishii, *Opt. Lett.* **26** (2001) p. 277.
71. Y. Cheng, K. Sugioka, K. Midorikawa, M. Masuda, K. Toyoda, M. Kawachi, and K. Shihoyama, *Opt. Lett.* **28** (2003) p. 55.
72. M. Masuda, K. Sugioka, Y. Cheng, N. Aoki, M. Kawachi, K. Shihoyama, K. Toyoda, H. Helvajian, and K. Midorikawa, *Appl. Phys. A* **76** (2003) p. 857.
73. Y. Bellouard, A. Said, M. Dugan, and P. Bado, *Opt. Express* **12** (2004) p. 2120.
74. K. Sugioka, Y. Cheng, and K. Midorikawa, *J. Photopolym. Sci. Technol.* **17** (2004) p. 397.
75. Y. Li, K. Itoh, W. Watanabe, K. Yamada, D. Kuroda, J. Nishii, and Y. Jiang, *Opt. Lett.* **26** (2001) p. 1912.
76. Y. Iga, T. Ishizuka, W. Watanabe, Y. Li, J. Nishii, and K. Itoh, *Jpn. J. Appl. Phys. Part 1* **43** (2004) p. 4207.
77. K. Ke, E.F. Hasselbrink Jr., and A.J. Hunt, *Anal. Chem.* **77** (2005) p. 5083.
78. T.N. Kim, K. Campbell, A. Groisman, D. Kleinfeld, and C.B. Schaffer, *Appl. Phys. Lett.* **86** 201106 (2005).
79. S.M. Eaton, H. Zhang, P.R. Herman, F. Yoshino, L. Shah, J. Bovatsek, and A.Y. Arai, *Opt. Express* **13** (2005) p. 4708.
80. A. Zoubir, M. Richardson, L. Canioni, A. Brocas, and L. Sarger, *J. Opt. Soc. Am. B* **22** (2005) p. 2138.
81. A. Szameit, D. Blömer, J. Burghoff, T. Schreiber, T. Pertsch, S. Nolte, A. Tünnermann, and F. Lederer, *Opt. Express* **13** (2005) p. 10552.
82. D.N. Christodoulides and E.D. Eugenieva, *Phys. Rev. Lett.* **87** 233901 (2001).
83. E.D. Eugenieva, N.K. Efremidis, and D.N. Christodoulides, *Opt. Lett.* **26** (2001) p. 1978.□

Advertisers in This Issue